*Recent Insights into the Physics of the Sun and Heliosphere*
*- Highlights from SOHO and Other Space Missions -*
*ASP Conference Series, Vol. 200, 2001*
*P. Brekke, B. Fleck, and J. B. Gurman eds.*

# Flare Occurrence in the Solar Active Regions with Reversed Helicity Sign

S.D. Bao, G.X. Ai, and H.Q. Zhang

*Beijing Astronomical Observatory/National Astronomical Observatories, Chinese Academy of Sciences, Beijing 100012, China*

**Abstract.** Based on the Huairou Solar Observing Station dataset, we computed the current helicity for several hundreds of active regions and found that: (1) Active regions that do not follow the hemispheric helicity sign rule show more flare activity than normal active regions. (2) The relative number of active regions with reversed helicity sign is higher near sunspot maximum. (3) It appears that during solar cycle 22 the southern hemisphere has more the reversed-sign active regions and stronger flare activity than the northern hemisphere.

## 1. Introduction

Observations have revealed that a hemispheric preference of net sign of helicity, or handedness, exists throughout the solar atmosphere — in the photosphere, the chromosphere, the corona, and the solar wind (e.g., Bao, Ai, & Zhang 2000; and references therein). In the photosphere more than 70% of active regions in the northern/southern hemisphere have negative/positive current helicity ($H_c$ or $\alpha$). Zhang and Bao (1999) have found the active regions with reversed helicity sign tend to emerge at certain longitudes. Current helicity of magnetic fields also plays an important role in solar flares (Pevtsov et al. 1995, 1996; Bao et al. 1999). Canfield et al. (1999) have classified active regions according to morphology (sigmoidal or non-sigmoidal) and nature of activity (eruptive or non-eruptive), and have found that regions are significantly more likely to be eruptive if they are either sigmoidal or large. The aim of this paper is to statistically examine whether active regions with abnormal helicity sign show more flare activity.

## 2. Data Analysis and Results

The data we used for this study were obtained with the vector video magnetograph at the Huairou Solar Observing Station of Beijing Astronomical Observatory. The detailed description of this instrumentation and the observational technique may be found elsewhere (Wang et al. 1996; Bao et al. 2000). All vector magnetograms were observed under good weather and seeing conditions during the time when the active regions were located near the central meridian.

Bao and Zhang (1998) used the same dataset to calculate current helicity of 422 active regions in the cycle 22. They found that 84% of the active regions

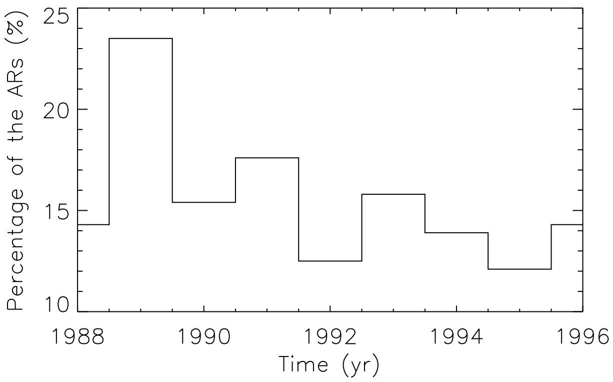


Figure 1. Distribution of the percentage of active regions that do not follow the helicity sign rule appeared on the solar disk with time.

in the northern hemisphere have negative helicity, and 79% in the southern hemisphere have positive helicity. The active regions that disobey this rule are listed in Table 1 including information on their flare activity. Most of the regions accompany by abundant flare activity. As a comparison, we also analyzed all active regions that follow the helicity sign rule, and found that active regions almost without flare activity amount to 25% of all normal active regions, but only 12% for the active regions with reversed helicity sign. In other words, these regions with reversed helicity sign have a tendency for enhanced flare activity.

Table 1 also shows that the number of active regions with reversed helicity sign reaches maximum near sunspot maximum (1989 and 1991), like other indicators of activity (such as flare count). Since the productivity of active regions is also high around sunspot maximum, we display a histogram of active regions with reversed helicity sign as a fraction of total number of active regions that appeared on the solar disk during the cycle 22 (Figure 1). This indicates that during the maximum years of solar activity the physical processes in deeper layers of the Sun are extremely complicated and dynamic, which leads to the emergence of a large number of tubes of different twisting, along with the appearance of relatively larger number of active regions with reversed helicity sign.

In addition, the north-south asymmetry can also be found in Table 1 from both the number of the reversed-sign active regions and the frequency of powerful flares occurred in these regions. Such a hemispheric asymmetry may be useful for understanding the physical conditions and processes deep below the photosphere. One should study further the relationship between flares and active regions with abnormal helicity using much larger dataset.

**Acknowledgments.** We are indebted to the staff of the Huairou Solar Observing Station for the observations. We also thank A.A. Pevtsov for his reading of this manuscript. This work is supported by National Science Foundation of China under grants 19791090 and 19973008.

Table 1. Synopsis of flare occurrence in the active regions with reversed helicity sign. 'l' — having some large flares exploded in an active region, 's' — only smaller flares occurred, 'm' — appearing many flares, 'f' — a few flares, and '-' — almost no flares.

| NOAA/AR | Date | Coordinate | $H_c$ | Flare class | Productivity |
|---|---|---|---|---|---|
| | | Northern hemisphere | | | |
| 5451 | 19 Apr., 1989 | N10 W05 | + | s | m |
| 5569 | 29 Jun., 1989 | N21 W04 | + | s | m |
| 5589 | 17 Jul., 1989 | N27 E04 | + | s | f |
| 5676 | 10 Sep., 1989 | N27 W02 | + | s | f |
| 5769 | 04 Nov., 1989 | N25 E05 | + | s | m |
| 5776 | 08 Nov., 1989 | N17 W01 | + | l | m |
| 5796 | 23 Nov., 1989 | N11 W05 | + | - | - |
| 5821 | 08 Dec., 1989 | N20 E04 | + | s | m |
| 6095 | 10 Jun., 1990 | N23 E00 | + | s | m |
| 6150 | 12 Jul., 1990 | N07 W06 | + | s | m |
| 6199 | 15 Aug., 1990 | N13 W04 | + | s | m |
| 6605 | 02 May , 1991 | N09 E01 | + | s | f |
| 6792 | 23 Aug., 1991 | N03 E01 | + | - | - |
| 6893 | 30 Oct., 1991 | N17 E02 | + | s | f |
| 6908 | 10 Nov., 1991 | N21 E05 | + | s | f |
| 7019 | 21 Jan., 1992 | N17 W02 | + | s | m |
| 7029 | 29 Jan., 1992 | N17 E01 | + | - | - |
| 7050 | 12 Feb., 1992 | N11 W02 | + | s | m |
| 7145 | 27 Apr., 1992 | N12 W04 | + | s | f |
| 7425 | 18 Feb., 1993 | N15 W03 | + | l | m |
| 7448 | 17 Mar., 1993 | N16 W04 | + | l | m |
| 7496 | 10 May , 1993 | N15 W06 | + | s | m |
| 7512 | 30 May , 1993 | N08 W05 | + | s | f |
| 7671 | 20 Feb., 1994 | N11 W04 | + | s | m |
| 7794 | 31 Oct., 1994 | N13 E05 | + | s | m |
| 7870 | 14 May , 1995 | N10 E02 | + | s | m |
| | | Southern hemisphere | | | |
| 5137 | 19 Aug., 1988 | S20 E00 | − | s | f |
| 5148 | 17 Sep., 1988 | S11 E03 | − | s | f |
| 5212 | 04 Nov., 1988 | S17 W06 | − | s | m |
| 5312 | 13 Jan., 1989 | S32 E04 | − | l | m |
| 5497 | 23 May , 1989 | S20 E01 | − | l | m |
| 5622 | 05 Aug., 1989 | S27 E01 | − | l | m |
| 5657 | 23 Aug., 1989 | S20 E08 | − | - | - |
| 5669 | 05 Sep., 1989 | S17 E01 | − | l | m |
| 5747 | 20 Oct., 1989 | S26 W01 | − | l | m |
| 5801 | 26 Nov., 1989 | S20 E00 | − | - | - |
| 5947 | 26 Feb., 1990 | S17 W04 | − | s | m |
| 6050 | 09 May , 1990 | S11 E03 | − | s | f |
| 6064 | 19 May , 1990 | S15 W01 | − | l | m |
| 6131 | 03 Jul., 1990 | S21 W02 | − | l | m |
| 6227 | 26 Aug., 1990 | S23 W02 | − | l | m |
| 6462 | 27 Jan., 1991 | S18 E06 | − | s | m |
| 6509 | 24 Feb., 1991 | S21 E03 | − | s | f |
| 6593 | 21 Apr., 1991 | S12 W06 | − | l | m |
| 6615 | 06 May , 1991 | S11 W04 | − | s | m |
| 6698 | 30 Jun., 1991 | S05 W04 | − | - | - |
| 6818 | 04 sep., 1991 | S12 W02 | − | l | m |
| 6873 | 15 Oct., 1991 | S23 W07 | − | s | m |
| 7026 | 27 Jan., 1992 | S13 E00 | − | s | f |
| 7039 | 04 Feb., 1992 | S15 W03 | − | l | m |

Table 1. — *Continued*

| NOAA/AR | Date | Coordinate | $H_c$ | Flare class | Productivity |
|---|---|---|---|---|---|
| 7335 | 12 Nov., 1992 | S18 W06 | – | s | f |
| 7345 | 23 Nov., 1992 | S24 W04 | – | l | m |
| 7400 | 13 Jan., 1993 | S09 W04 | – | s | m |
| 7411 | 26 Jan., 1993 | S12 E01 | – | s | m |
| 7493 | 04 May , 1993 | S10 W03 | – | s | f |
| 7563 | 17 Aug., 1993 | S04 W04 | – | s | m |
| 7625 | 30 Nov., 1993 | S15 W01 | – | - | - |
| 7629 | 08 Dec., 1993 | S21 E00 | – | s | m |
| 7742 | 03 Jul., 1994 | S09 E00 | – | s | f |
| 7792 | 24 Oct., 1994 | S08 E04 | – | s | f |
| 7815 | 14 Dec., 1994 | S11 W05 | – | l | m |
| 7842 | 20 Feb., 1995 | S14 E06 | – | - | - |
| 7854 | 21 Mar., 1995 | S17 W02 | – | s | m |
| 7921 | 12 Nov., 1995 | S10 E01 | – | s | f |
| 7999 | 26 Nov., 1996 | S05 E05 | – | s | m |

## References


Bao, S. D., Ai, G. X., & Zhang, H. Q. 2000, J. Astrophys. Astr., in press

Bao, S. D., Pevtsov, A. A., Wang, T. J., & Zhang, H. Q. 2000, Solar Phys., 195, 75

Bao, S. D. & Zhang, H. Q. 1998, ApJ, 496, L43

Bao, S. D., Zhang, H. Q., Ai, G. X., & Zhang, M. 1999, A&AS, 139, 311

Canfield, R. C., Hudson, H. S., & McKenzie, D. E. 1999, Geophysical Research Letters, 26, 627

Pevtsov, A. A., Canfield, R. C., & Metcalf, T. R. 1995, ApJ, 440, L109

Pevtsov, A. A., Canfield, R. C., & Zirin, H. 1996, ApJ, 473, 533

Zhang, H. Q. & Bao, S. D. 1999, ApJ, 519, 876

Wang J. X., Shi Z. X., Wang H. N., & Lü Y. P. 1996, ApJ, 456, 861